Overview of Low-speed Aerodynamic Tests on a 5.75% Scale Blended-Wing-Body Twin Jet Configuration

Dan D. Vicroy*
NASA Langley Research Center, Hampton, Virginia 23681, USA

Eric Dickey†, Norman Princen‡ and Michael D. Beyar§
The Boeing Company, Huntington Beach, CA, 92647

The NASA Environmentally Responsible Aviation (ERA) Project sponsored a series of computational and experimental investigations of the propulsion and airframe integration issues associated with Hybrid-Wing-Body (HWB) or Blended-Wing-Body (BWB) configurations. NASA collaborated with Boeing Research and Technology (BR&T) to conduct this research on a new twin-engine Boeing BWB transport configuration. The experimental investigations involved a series of wind tunnel tests with a 5.75-percent scale model conducted in two low-speed wind tunnels. This testing focused on the basic aerodynamics of the configuration and selection of the leading edge Krueger slat position for takeoff and landing. This paper reviews the results and analysis of these low-speed wind tunnel tests.

Nomenclature

q	=	dynamic pressure
α	=	angle of attack
β	=	angle of sideslip
δ_{LE}	=	leading edge Krueger deflection
η	=	fraction of semi-span
C_A	=	axial force coefficient
C_D	=	drag force coefficient
C_L	=	lift force coefficient
C_l	=	rolling moment coefficient
C_{l_β}	=	$\partial C_l/\partial\beta$
C_m	=	pitching moment coefficient
C_N	=	normal force coefficient
C_n	=	yawing moment coefficient
C_{n_β}	=	$\partial C_n/\partial\beta$
C_Y	=	side force coefficient
C_{Y_β}	=	$\partial C_Y/\partial\beta$
P	=	rake probe total pressure
P_T	=	tunnel total pressure
V	=	velocity

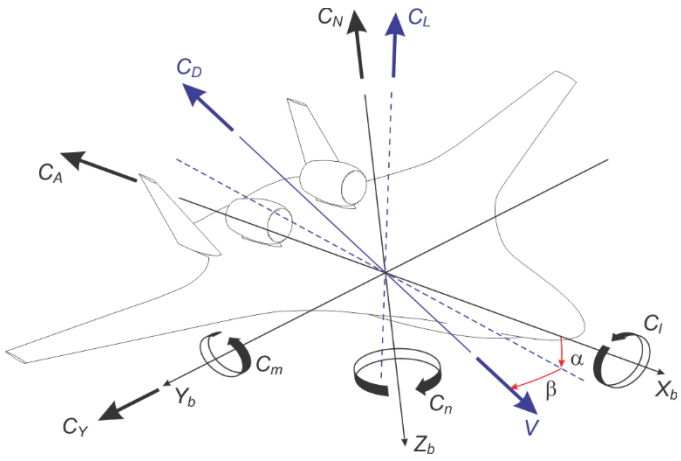

* Senior Researcher, Flight Dynamics Branch, Research Directorate, MS 308, Associate Fellow, AIAA
† Senior Engineer, Aerosciences, Flight & Vehicle Technology, Boeing Research & Technology, 14900 Bolsa Chica St, Huntington Beach CA, 92647, AIAA Non-member
‡ Senior Engineer, Vehicle Control & Dynamics , Flight & Vehicle Technology, Boeing Research & Technology, 14900 Bolsa Chica St, Huntington Beach CA, 92647, AIAA Senior Member
§ Aerodynamics Engineer, Flight & Vehicle Technology, Boeing Research & Technology, 14900 Bolsa Chica Rd., Huntington Beach CA, 92647, AIAA Member

Introduction

THE NASA Environmentally Responsible Aviation (ERA) Project within the Integrated Systems Research Program (ISRP) of the Aeronautics Research Mission directorate (ARMD) sponsored a series of computational and experimental investigations of the propulsion and airframe integration issues associated with Hybrid-Wing-Body (HWB) or Blended-Wing-Body (BWB) configurations. Of the various advanced configurations studied within the program, the HWB has shown the unique potential of simultaneously achieving the ERA combined N+2 goals for noise, fuel efficiency and emissions[1]. Because of this potential, the ERA Project has been interested in reducing the technology risks associated with the HWB concept. One of the identified technology risk areas is the propulsion and airframe integration. The location of the engines on the aft upper surface of the HWB centerbody contributes to the noise shielding benefit of the configuration. However, it also poses some unique propulsion and airframe integration challenges.

NASA collaborated with Boeing Research and Technology (BR&T) to conduct this research on a new twin-engine Boeing BWB transport configuration. The experimental investigations involved a series of wind tunnel tests with a 5.75-percent scale model conducted in two low-speed wind tunnels, as shown in Figures 1 and 2. These wind tunnel tests were comprised of three distinct test configurations; a flow-thru nacelle test configuration, an ejector test configuration and a turbine propulsion-simulator configuration. As the name implies, the flow-thru nacelle tests used flow-thru engine nacelles on the model. This testing focused on the basic aerodynamics of the configuration and selection of the leading edge Krueger slat position for takeoff and landing. The ejector test use high-pressure air ejectors in the nacelles to generate the desired inlet mass-flow conditions necessary for inlet distortion analysis. The turbine propulsion-simulator tests used high-pressure turbine engine simulators to generate the desired engine exit flow to study the interaction of the engine jet exhaust with the aft body aerodynamics and control surfaces. This paper reviews the results and analysis of the flow-thru nacelle phase of the testing.

Experimental Setup

A. Model Description

The model is a 5.75-percent geometrically scaled version of the Boeing Blended-Wing-Body BWB-0009G configuration. A three-view drawing of the model is shown in Fig. 3. The model was fabricated of aluminum and had a fully instrumented test weight of approximately 1250 pounds.

Fig. 1. 5.75% scale BWB-0009G model in the 14- by 22-Foot Tunnel with walls and ceiling down.

Fig. 2. 5.75% scale BWB-0009G model in the NFAC 40- by 80-Foot Tunnel.

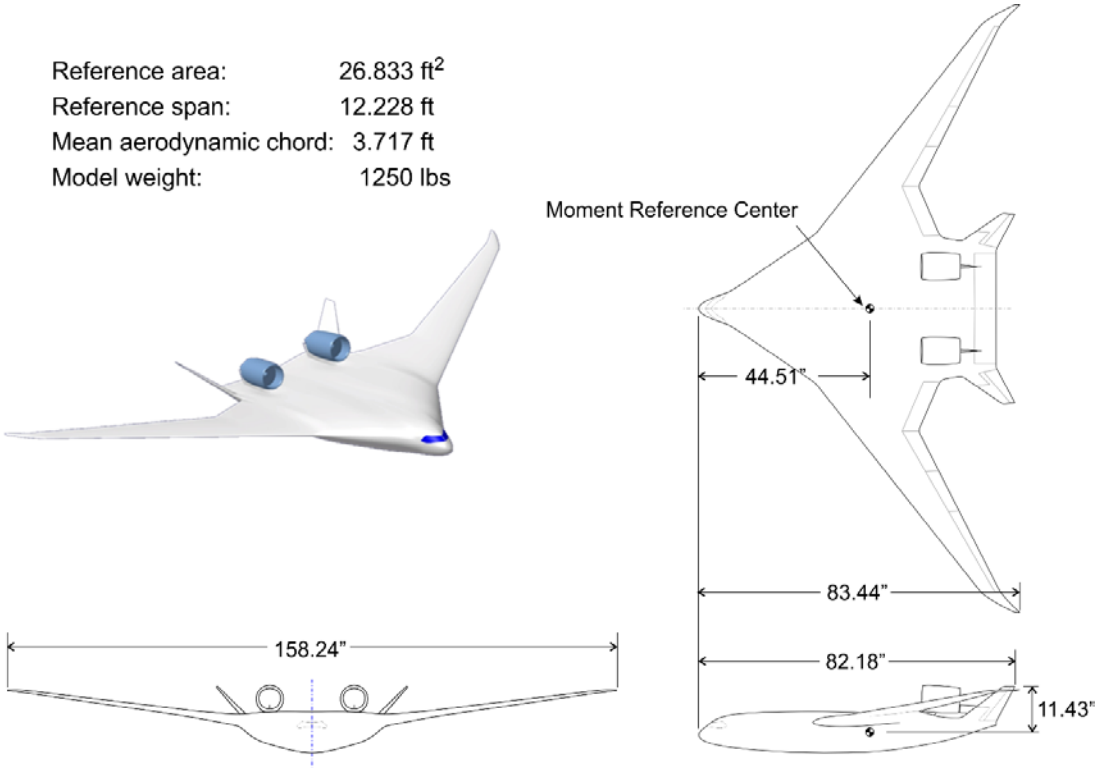

Fig. 3. Three-view drawing of 5.75-percent scale BWB-0009G model.

The model has thirteen control surfaces distributed along the trailing edge and vertical tails of the vehicle as illustrated in Fig. 4. The outboard elevons (elevon 6/7) have an upper and lower surface that can be split to provide directional control as a drag rudder or deflected as a standard elevon. The vertical tails are deflectable and have additional ruddervator panels along their trailing edge. All the control deflection angles were measured streamwise with positive elevon deflections being trailing edge down and positive rudder deflections are trailing edge left. Due to time constraints only a limited set of the fixed deflection angles available for each control surface were tested.

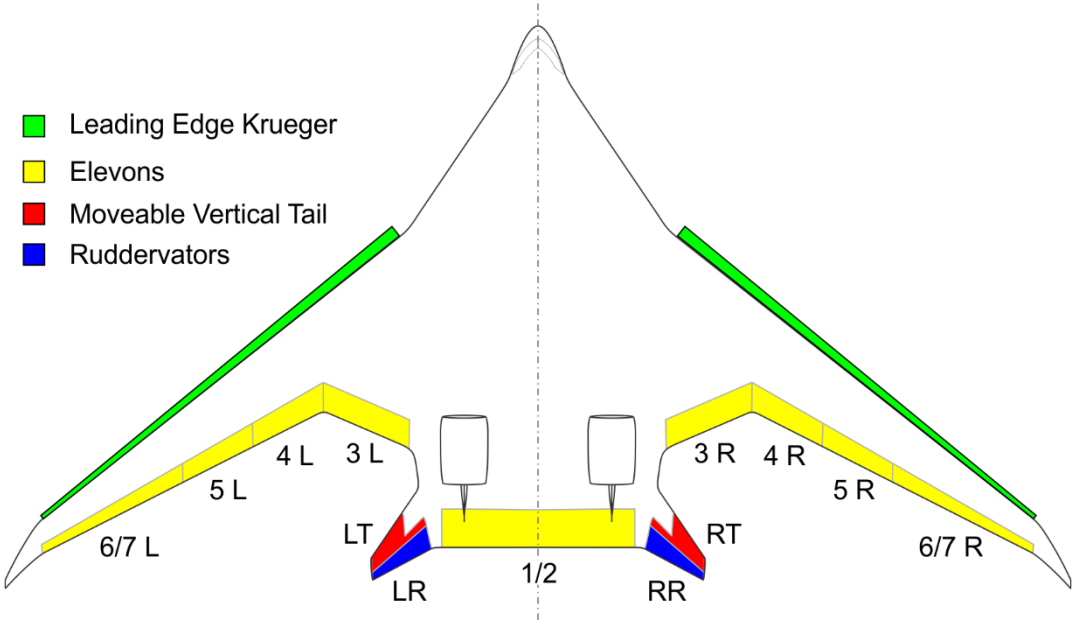

Fig. 4. Model control surfaces.

The high-lift system for the model consisted of a leading edge Krueger slat extending along the extent of the outboard wing section. The Krueger position could be varied in deflection angle, gap and overhang, which were set by five mounting brackets on each wing (Fig 5). Mounting brackets were provided for takeoff position deflections of 30°, 35° and 40° and landing position deflections of 40°, 45° and 50°. A 2x2 grid of available gap and overhang positions were provided for the takeoff positions and a 3x3 grid for the landing, as illustrated in Fig. 6. In addition to the position and deflection options, two leading edge Krueger shapes were also tested. The "Baseline" Krueger was the original Krueger concept and the configuration with which the majority of the pre-test CFD was conducted. The "Acoustic" Krueger was developed as a more realistic profile and was the configuration with which the majority of the wind tunnel testing was conducted. All of the Krueger wind tunnel data presented in this report is with the "Acoustic" geometry unless specifically noted otherwise.

Nine 15 psi pressure modules were used to measure pressures at various locations on the model. The 311 pressure tap locations on the upper and lower surface of the model are illustrated in Fig. 7. There were also 127 pressure taps located on the inner and outer surface of the left nacelle/pylon. The right nacelle included a 40-probe pressure rake, as shown in Fig. 8, to measure inlet distortion.

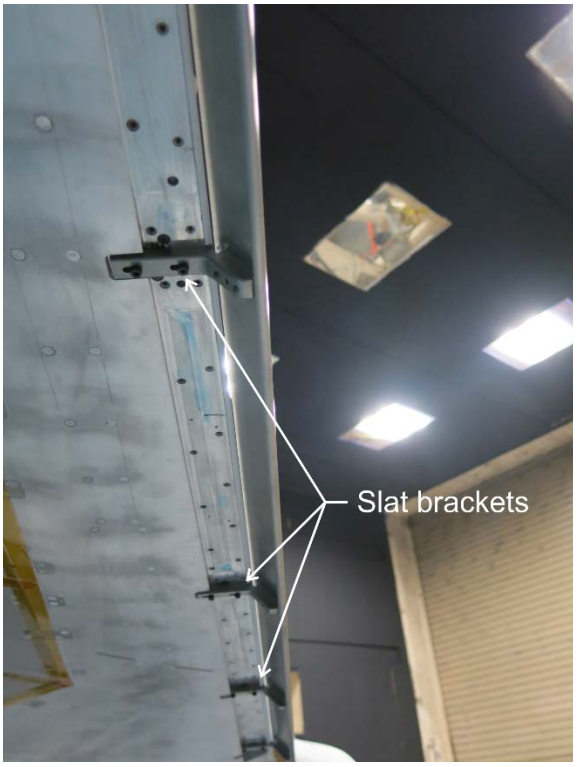

Fig. 5. Deflected leading-edge Krueger and mounting brackets or right wing.

Force and moment measurements were obtained with an internal flow-thru six-component strain gauge balance. The first two tests (LaRC T617 and NFAC T078) used a new balance designated MC-126-6Ai. The third test (NFAC T378) used the Ames 6" flow-thru balance No. 1 [2]. Both of these balances are 5x1 flow-thru force balances which resolve component loads consisting of five forces and one moment. The five forces consist of two normal forces, two side forces and one axial force. The rolling moment is measured whereas the pitching moment and yawing moment are resolved from the difference between the normal and side force pair, respectively, and the distance between the strain gauges.[3] The maximum load range and calibration accuracy (± 1 standard deviation) for the two balances are listed in Table 1. The full load range and flow-thru capability of balance MC-126-6Ai was not required for the testing reported here but was chosen for the subsequent testing that included the pneumatic turbine engine simulators.

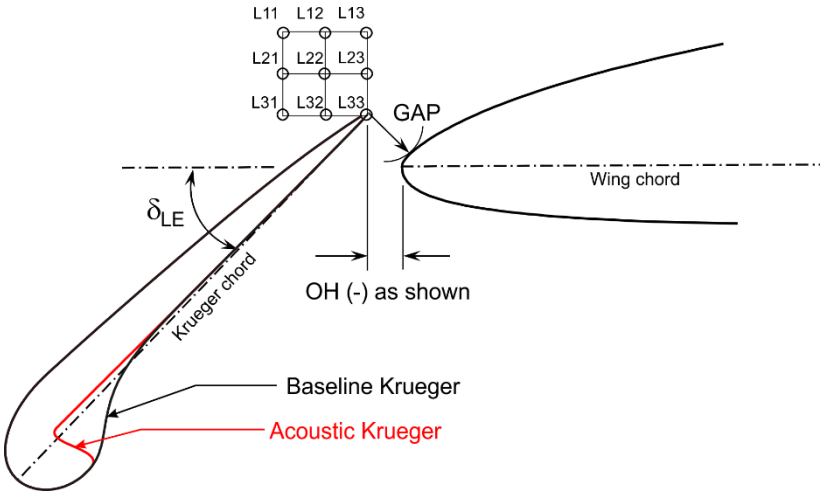

Fig. 6. Krueger profiles and landing Krueger gap and overhang (OH) positions.

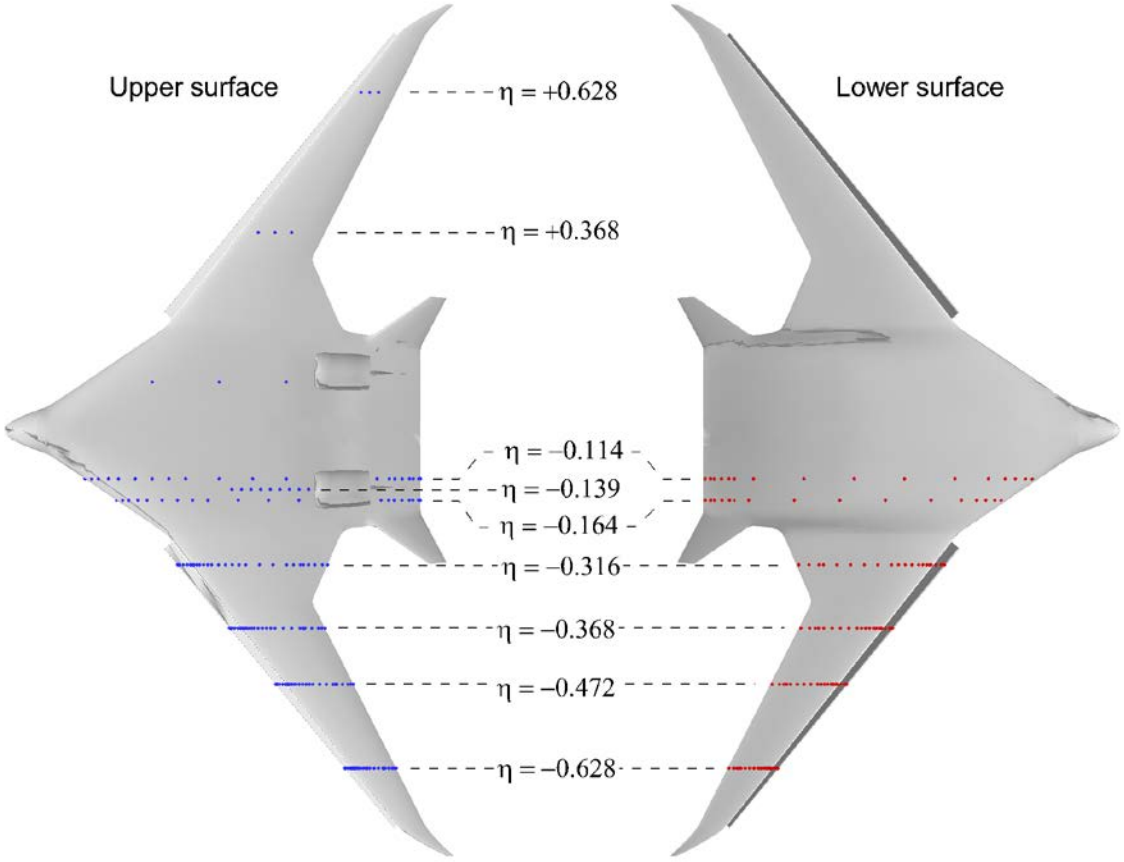

Fig. 7. Upper and lower surface pressure tap locations.

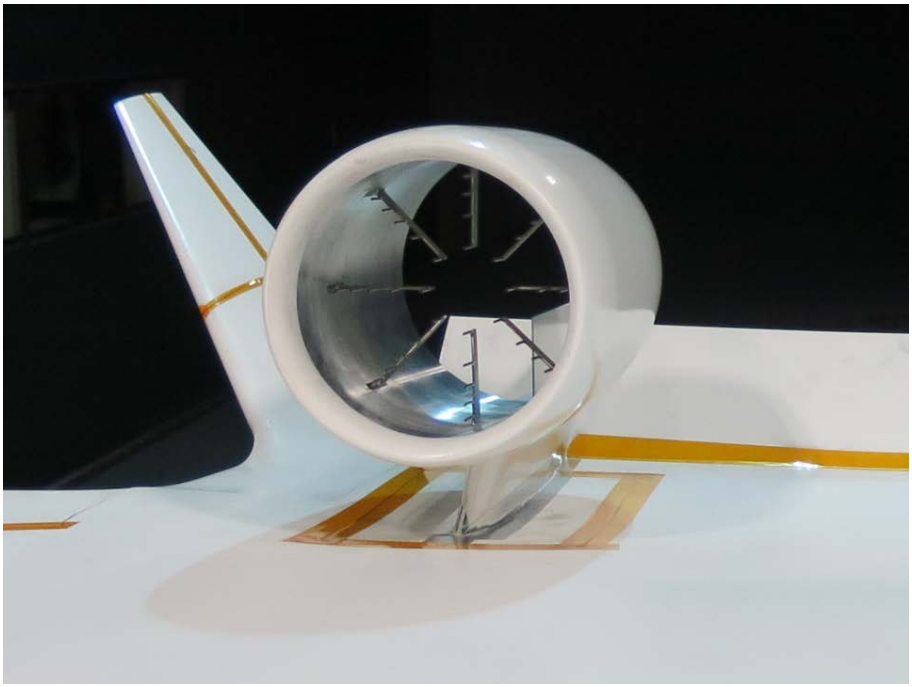

Fig. 8. Right nacelle pressure rake.

Table 1. Internal balance load capacities.

	MC-126-6Ai			Ames 6” flow-thru No. 1		
	Max load	Std. Dev.	% max	Max load	Std. Dev.	% max
Normal Force	±12,600 lbs	3.373 lbs	0.0268	±3,400 lbs	2.322 lbs	0.0683
Pitching Moment	±44,100 in-lbs	26.115 in-lbs	0.0592	±18,700 in-lbs	12.773 in-lbs	0.0683
Side Force	±9,200 lbs	3.224 lbs	0.0701	±2,200 lbs	2.084 lbs	0.0947
Yawing Moment	±32,200 in-lbs	14.628 in-lbs	0.0454	±12,100 in-lbs	11.465 in-lbs	0.0947
Rolling Moment	±35,000 in-lbs	42.253 in-lbs	0.1207	±7,200 in-lbs	38.993 in-lbs	0.5416
Axial Force	±1,400 lbs	2.046 lbs	0.1461	±1,400 lbs	1.052 lbs	0.0752

B. Test Facilities

The first series of wind tunnel tests were conducted in the 14- by 22-Foot Subsonic Tunnel at the NASA Langley Research Center. An aerial view of the facility is shown in the photograph presented in Fig. 9. This facility is a closed-circuit, single-return, atmospheric wind tunnel capable of producing a maximum speed of 348 feet per second. The testing was primarily conducted at a fixed dynamic pressure of 60 psf or approximately 233 feet per second. The facility can also be operated in either an open configuration (floor only, no walls or ceiling), as shown in Fig. 10, or a closed test-section configuration (i.e., walls and ceiling down), as shown in Fig. 1. The majority of the results presented in this paper are from measurements with the closed test-section configuration. Any data collected with the open configuration will be noted accordingly. Further tunnel details and facility information are available in Ref. 4.

A fan drive issue in the 14- by 22-Foot Tunnel resulted in the testing being moved to the U. S. Air Force National Full-Scale Aerodynamics Complex (NFAC) located at NASA Ames Research Center shown in Fig. 11. The tests were conducted in the NFAC 40- by 80-foot test section as seen in Fig. 2. The bulk of this testing was also conducted at a fixed dynamic pressure of 60 psf.

Fig. 9. Aerial view of the NASA Langley 14- by 22-Foot Subsonic Tunnel.

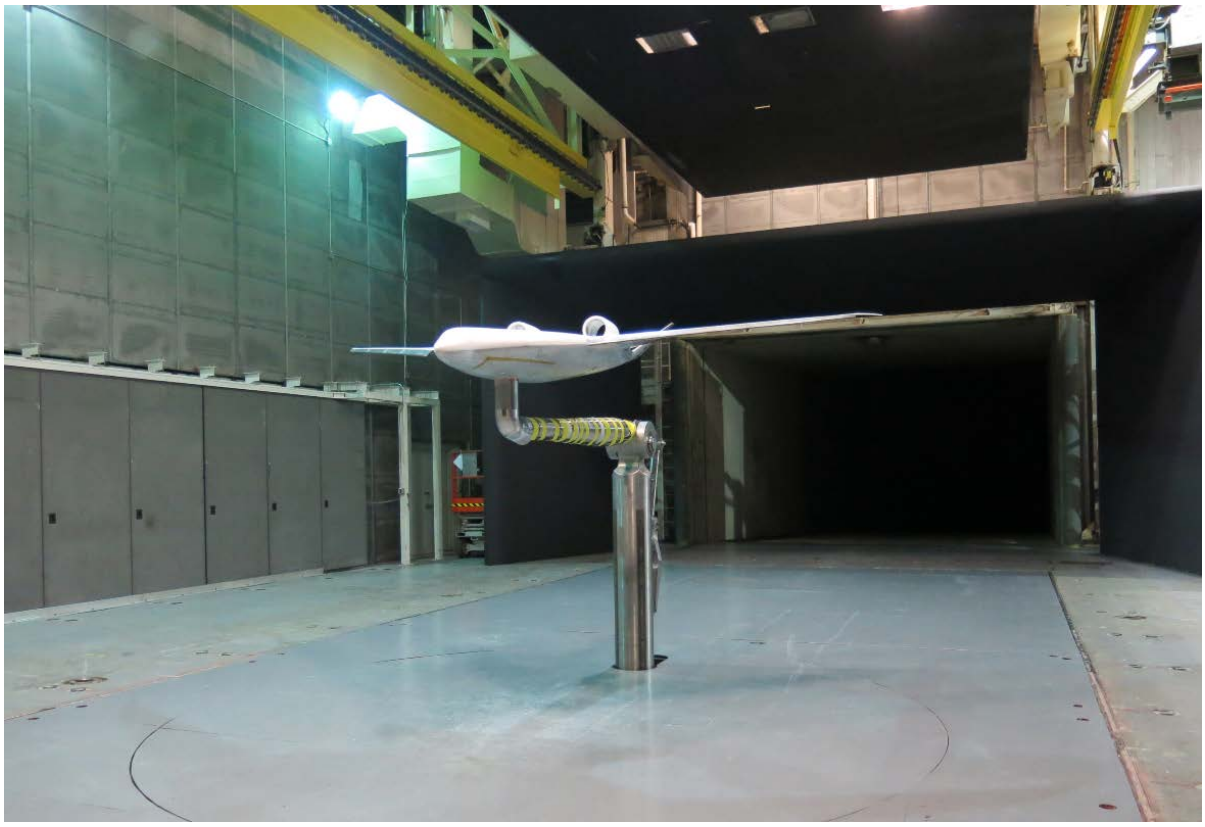

Fig. 10. BWB-0009G model in the 14- by 22-Foot Tunnel with walls and ceiling raised.

Fig. 11. Aerial view of the NFAC 40- by 80-Foot Subsonic Tunnel at NASA Ames Research Center.

C. Test Matrix

A general outline of the test matrices for the LaRC 14x22 and NFAC 40x80 test entries are listed in table 2. The extent of the available test data exceeds what can be presented within this paper.

Table 2. Test condition matrix.

LaRC 14x22 Test 617
Cruise Configuration
Baseline aero data: α sweeps at β = 0° / α sweeps at -20°≤ β ≤ +20°
Baseline aero data: β sweeps at α = 5°, 10°, 15°
Effect of q variation q = 10, 20, 40, 60 psf
Effect of upper & lower surface leading edge transition strips
Takeoff Configuration with Acoustic Krueger
Leading edge Krueger optimization runs (α sweeps with δ_{LE} = 30°, 35°, 40°)
Effect of q variation q = 10, 20, 40, 60 psf with δ_{LE} = 40° 1,1
Landing Configuration with Acoustic Krueger
Leading edge Krueger optimization runs (α sweeps with δ_{LE} = 40°, 45°, 50°)
Effect of elevon 1/2 trim deflection
Effect of walls up / walls down
Effect of upper & lower surface leading edge transition strips
Effect of Krueger dummy brackets
Effect of q variation q = 10, 20, 40, 60 psf with δ_{LE} = 50° 3,3
Landing Configuration with Baseline Krueger
Baseline aero data: α sweeps at β = 0° / β sweeps at α = 10°
Effect of Krueger stowage well covers
NFAC 40x80 Test 078
Cruise Configuration
Baseline aero data: α sweeps at β = 0° / α sweeps at -20°≤ β ≤ +20°
Effect of q variation q = 20, 40, 60, 90 psf
Effect of data sampling duration
Takeoff Configuration with Acoustic Krueger δ_{LE} = 40° 1,1
Baseline aero data: α sweeps at β = 0° / α sweeps at -15°≤ β ≤ +20°
Effect of q variation q = 10, 20, 40, 60 psf
Landing Configuration with Acoustic Krueger δ_{KR} = 45° 3,2
Baseline aero data: α sweeps at β = 0° / α sweeps at -20°≤ β ≤ +20°
Effect of elevon deflection (left side only)
Effect of Krueger dummy brackets
Effect of q variation q = 20, 40, 60 psf
NFAC 40x80 Test 378
Cruise Configuration
Baseline aero data: α sweeps at β = 0° / α sweeps at -5°≤ β ≤ +5°
Effect of q variation q = 20, 40, 60, 90 psf
Takeoff Configuration with Acoustic Krueger δ_{LE} = 40° 1,1
Baseline aero data: α sweeps at β = 0° / α sweeps at -20°≤ β ≤ +20°
Takeoff Configuration with Acoustic Krueger δ_{LE} = 40° 2,2 with sealed slot
Baseline aero data: α sweeps at β = 0°, 5° and 20°
Effect of elevon 1/2 trim deflection
Effect of rudder and vertical tail pitch deflection at β = 0°, 5°
Landing Configuration with Acoustic Krueger δ_{LE} = 45° 3,2
Baseline aero data: α sweeps at β = 0° / α sweeps at -20°≤ β ≤ +20°
Landing Configuration with Acoustic Krueger δ_{LE} = 50° 3,3 with sealed slot
Baseline aero data: α sweeps at β = 0° / α sweeps at -20°≤ β ≤ +20°
Effect of landing elevon deflection (elevons 3-5 = 10°, elevon 1/2 = -20°)

D. Test Data Corrections

This test took advantage of available pre-test CFD resources to explore and compare the "classic" wind tunnel test corrections with CFD predictions of the tunnel installation effects. The test corrections are applied to correct for blockage effects, buoyancy effects, strut interference effects and stream curvature effects[5,6]. Both the CFD based corrections and the classic corrections used the same correction methodology and equations. Only the correction parameter values differed. The CFD based parameters were established based on a least-squares fit of the parameter values that best matched the CFD predicted corrections. The CFD based corrections were only available for the 14x22 tunnels results. Consequently, the test results presented throughout the paper will be the classically corrected values unless explicitly stated otherwise.

Results and Discussion

A. Data Quality

1. Test correction comparison

A series of tests of the same model configuration in the 14x22 tunnel with the open and closed test-section provided an opportunity to compare the classic and CFD based corrections. The correction methods are intended to correct the data for tunnel installations effects and provide "free-air" aerodynamic measurements. The corrected data from the open and closed tunnel measurements of the same model configuration should therefore overlay each other. Figure 12 shows a comparison of uncorrected longitudinal force and moment data from a series of open and closed test sections runs with the same landing Krueger model configuration. The differences are most evident in the lift and drag at the higher angles of attack. Figures 13 and 14 show the same data sets corrected with the classic and CFD based values, respectively. Both methods provide an improvement in the matching of the open and closed tunnel measurements. The CFD based corrections were expected to provide a better match than the classic method. A closer examination of the matching is provided in Fig. 15, which shows the difference from the average of the three closed test section runs. The figure shows that the match provided by CFD based corrections were no better and in some cases worse than the classic corrections. Additional post-test CFD analysis including the NFAC test configuration comparison should provide greater insight into the test corrections and is worthy of further investigation.

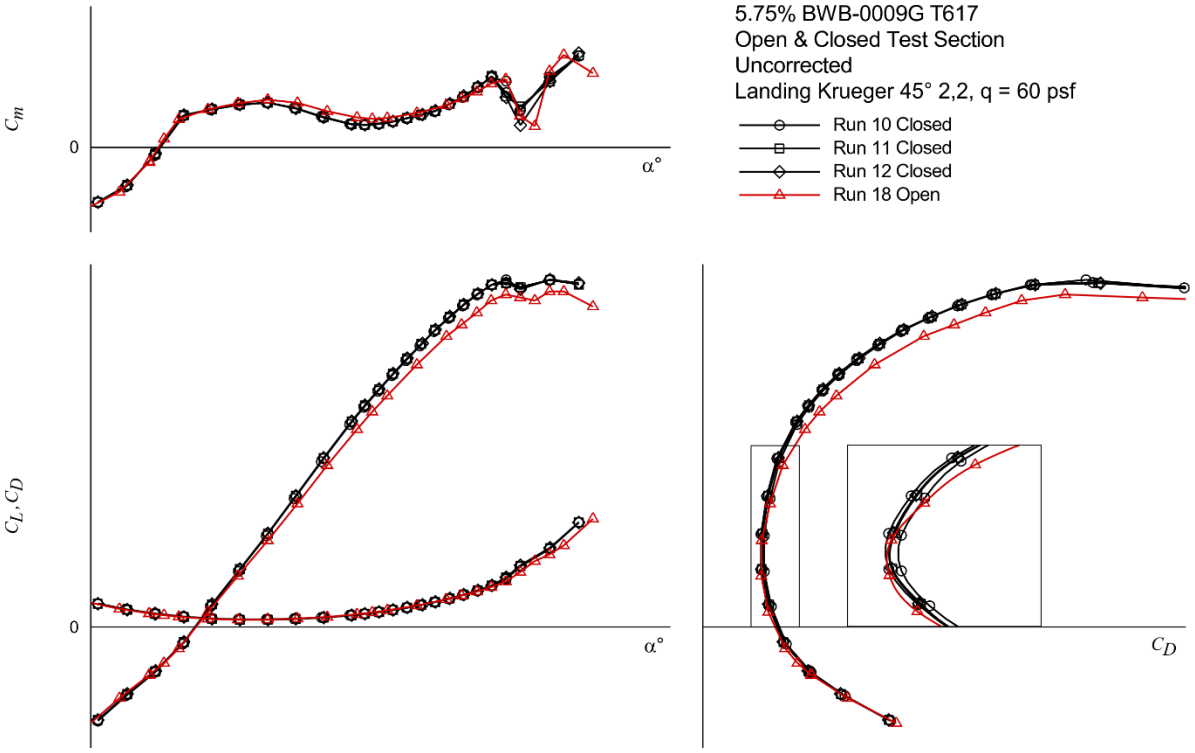

Fig. 12. Comparison of uncorrected open- and closed-tunnel longitudinal force and moment data of a landing Krueger configuration.

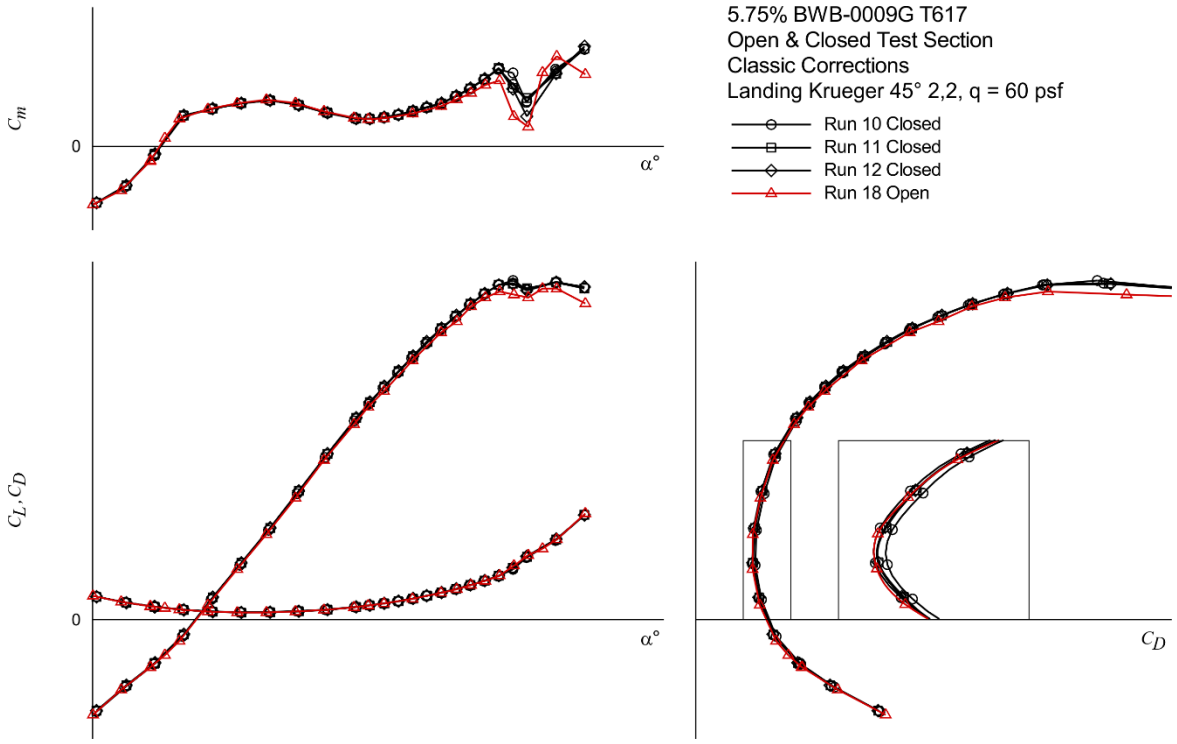

Fig. 13. Comparison of classic corrected open- and closed-tunnel longitudinal force and moment data of a landing Krueger configuration.

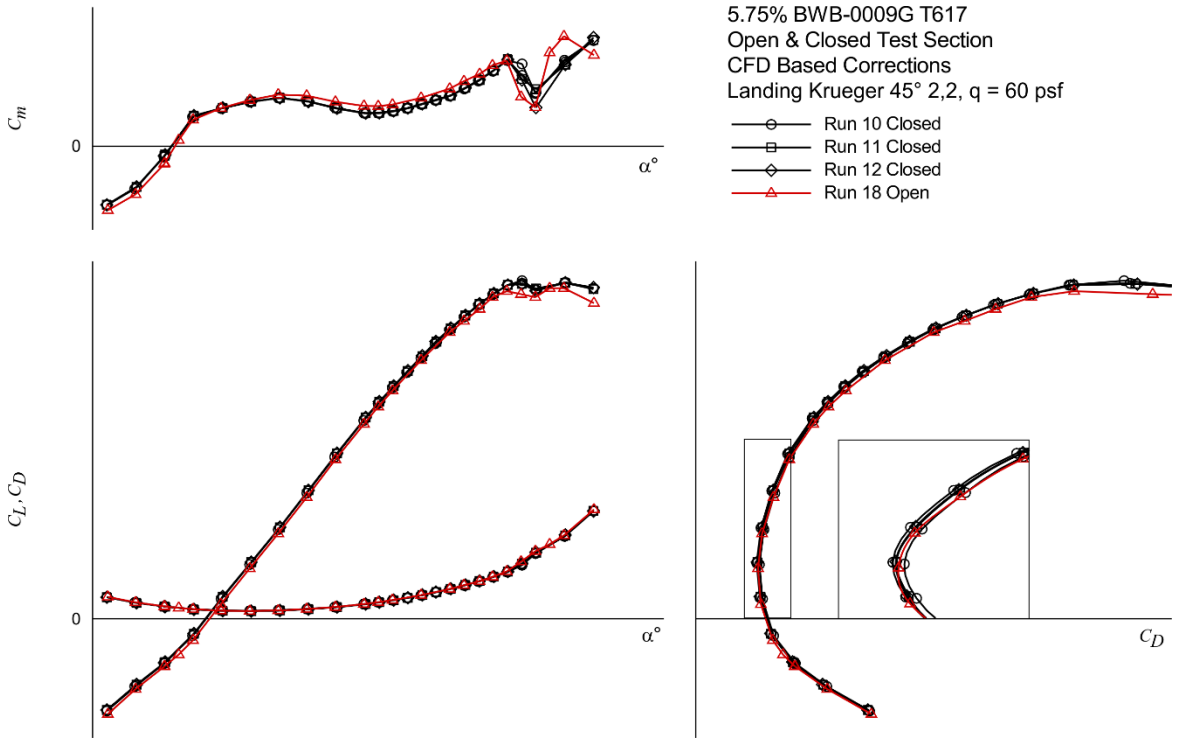

Fig. 14. Comparison of CFD corrected open- and closed-tunnel longitudinal force and moment data of a landing Krueger configuration.

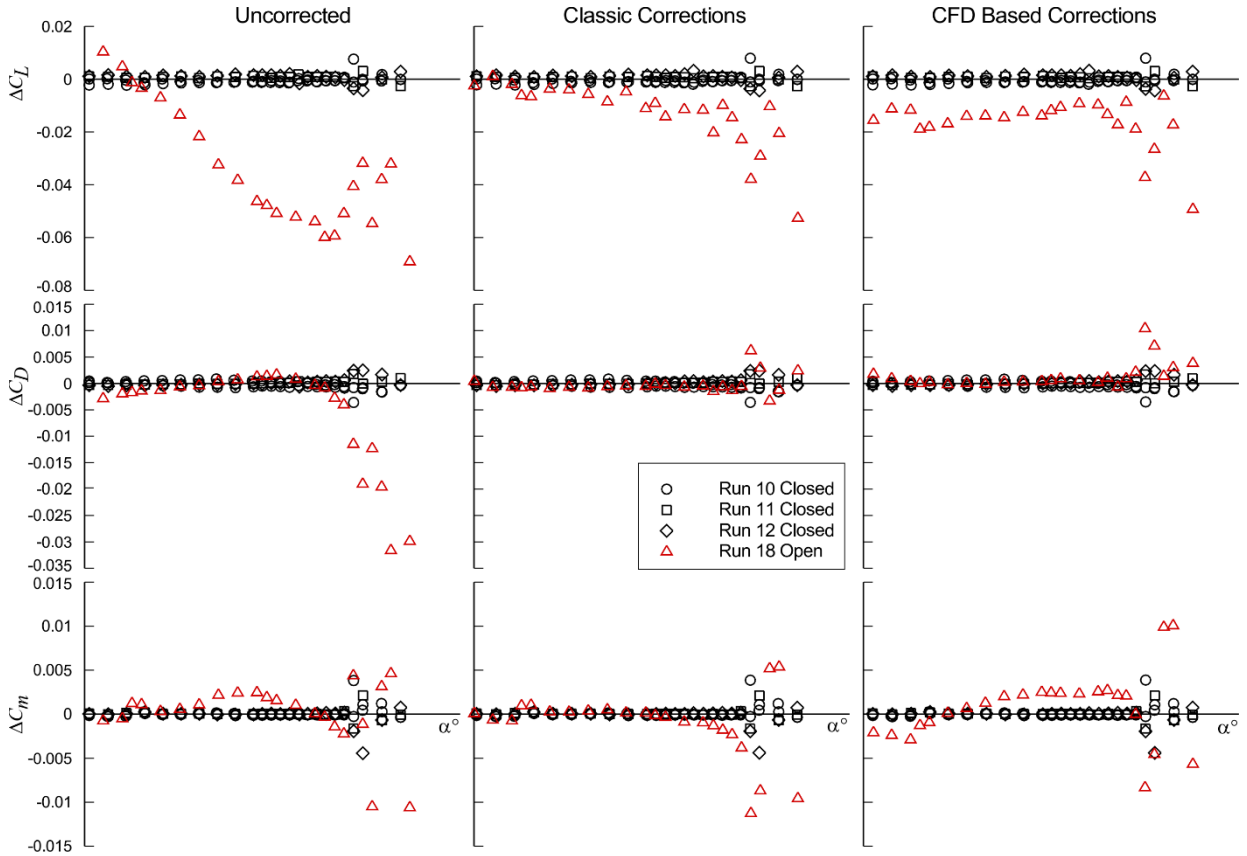

Fig. 15. Comparison of the difference from the average of the three closed test section runs.

2. Test to Test comparison

Three different tests were conducted with the 5.75% BWB-009G model in two different wind tunnels. The two tests in the same wind tunnel used different internal strain gauge balances and the two tests with the same balance were in different tunnels. Three common configurations were tested in all three wind tunnel test entries. Those were the Cruise configuration, the 45° 3,2 landing Krueger configuration, and the 40° 1,1 takeoff Krueger configuration. Figure 16 shows and comparison measured longitudinal forces and moments of the 45° 3,2 landing Krueger configuration from the three tests. The most apparent difference is the increased pitching moment of the NFAC tests and the increased minimum drag observed in T078.

In an effort to provide a more comprehensive test-to-test comparison, all coefficient measurements of the common configuration runs were interpolated to common angle of attack values and plotted against each other, as shown in Figures 17 and 18. Only angle of attack values below 21° were used to avoid comparing separated flow values, which can have large variations. Fig. 17 shows the common force and moment measurements of LaRC T617 verses those of NFAC T078. Both tests used the same model, sting and internal balance. Also shown on the figure is a least-squares liner fit of the data. A perfect replication of the data between tests would produce a linear fit with a slope of 1.0 and an intercept of 0. The figure shows good tunnel-to-tunnel agreement between the lift, drag and rolling moment values. There was a slight difference in the side force and yawing moment values. The Cruise configuration was the only common non-zero sideslip configuration between these two tests and the resultant side force and yawing moment values were small. The pitching moment showed the largest difference between the tests. The linear fit shows that the pitching moment in NFAC T078 was about a 10% larger than LaRC T617. This small difference may be due to differences in the tunnel test corrections between the tunnels and will be explored further with CFD.

Figure 18 shows the common force and moment measurements of NFAC T078 verses those of NFAC T378. These tests differed only by the internal balance used. NFAC T078 used the new MC-126-6Ai balance whereas NFAC T378 used the lower capacity Ames 6” flow-thru No. 1. All three forces and the rolling moment compare well. However, the pitch and yaw moment values differ between 15 and 20-percent indicating that there may be an error in the gauge distances used for one of the balances. The balances are currently being recalibrated in an effort to resolve this issue.

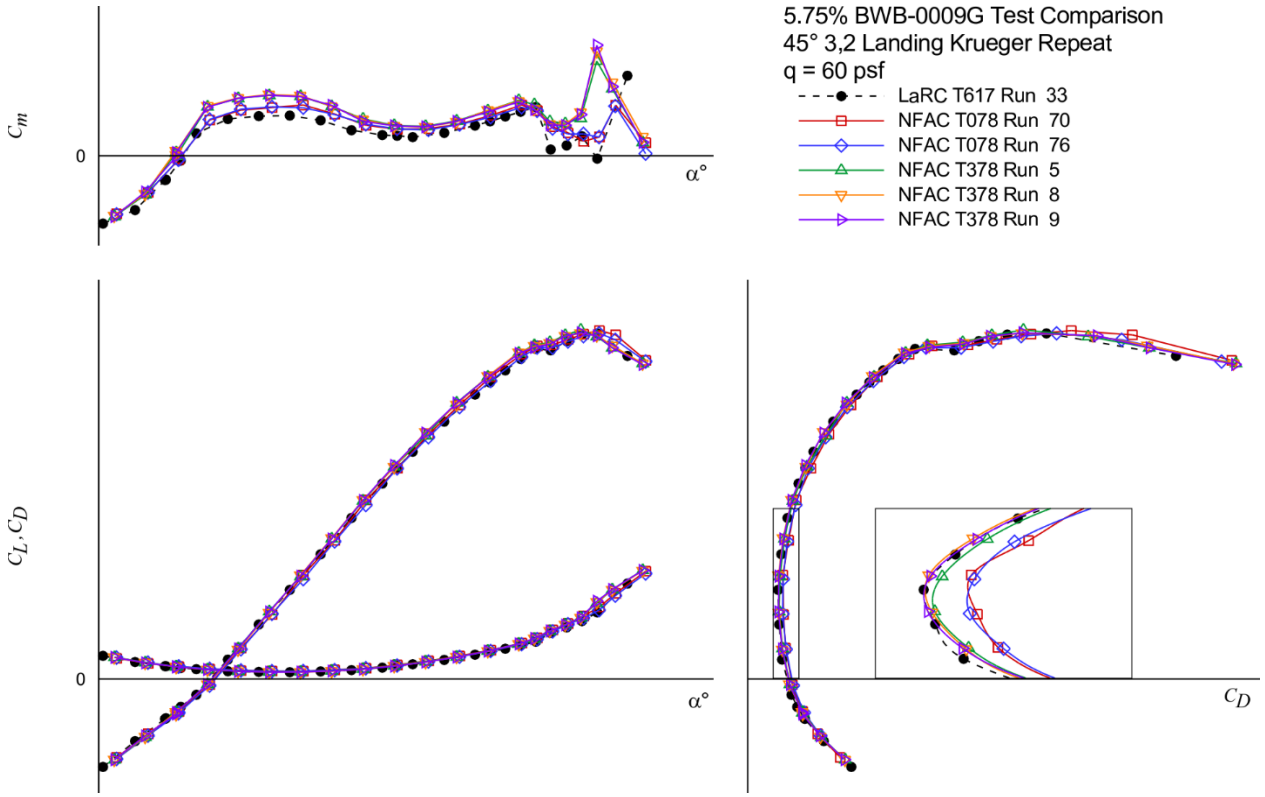

Fig. 16. Test to test comparison of the 45° 3,2 landing Krueger longitudinal measurements.

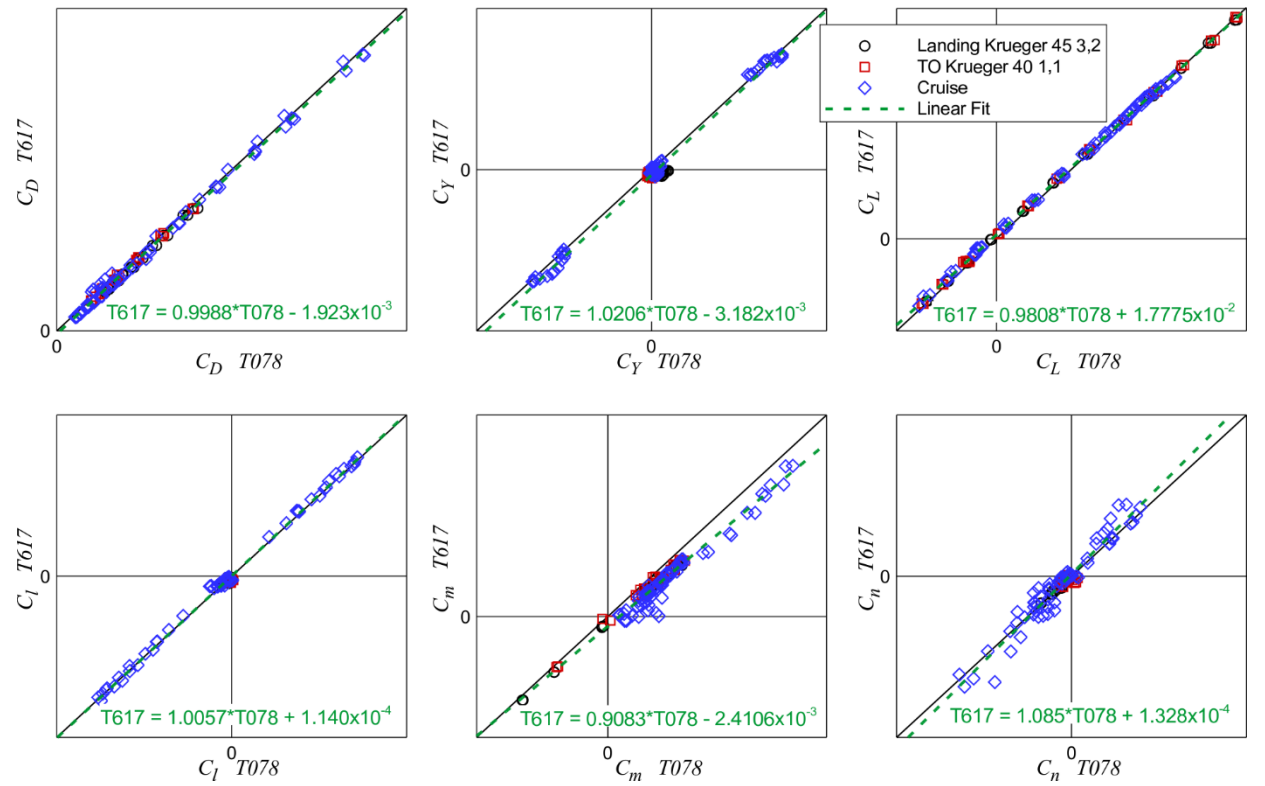

Fig. 17. Common configuration data comparison from tests with the same internal balance in different tunnels.

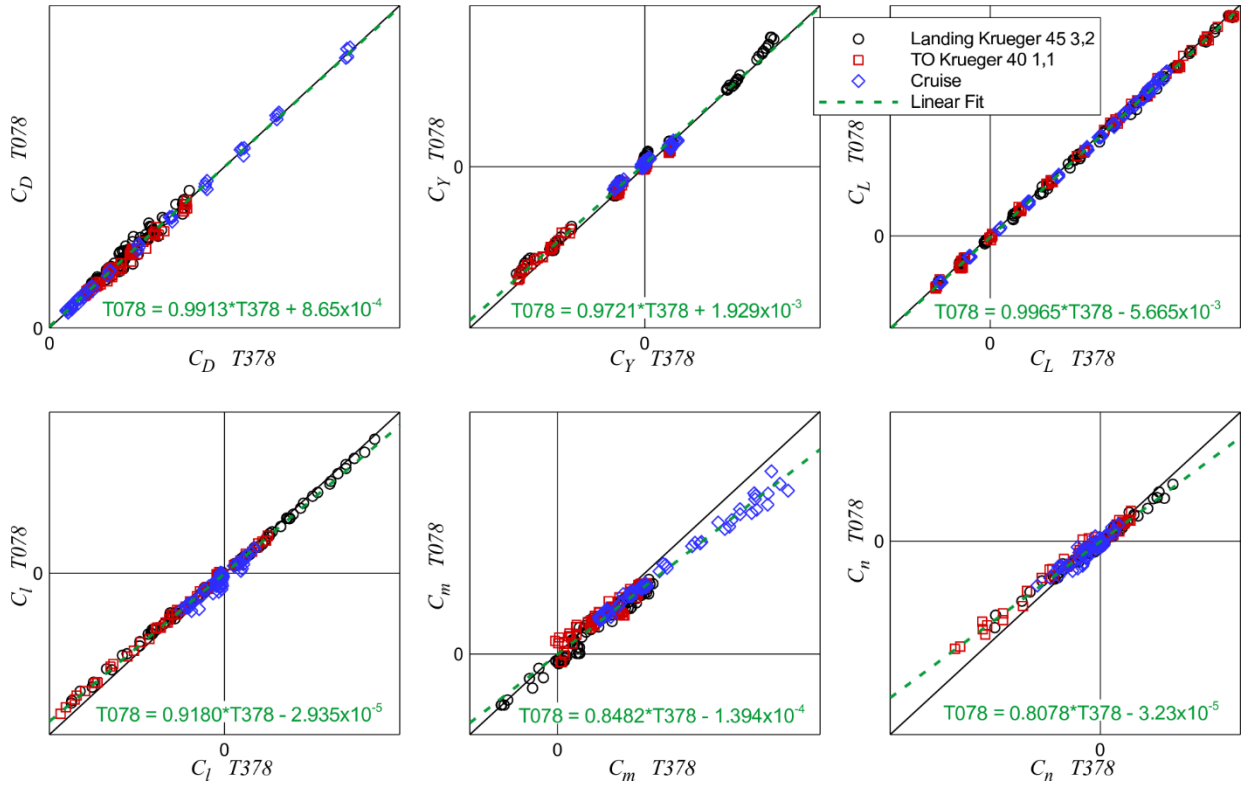

Fig. 18. Common configuration data comparison from tests in the same tunnel with different internal balances.

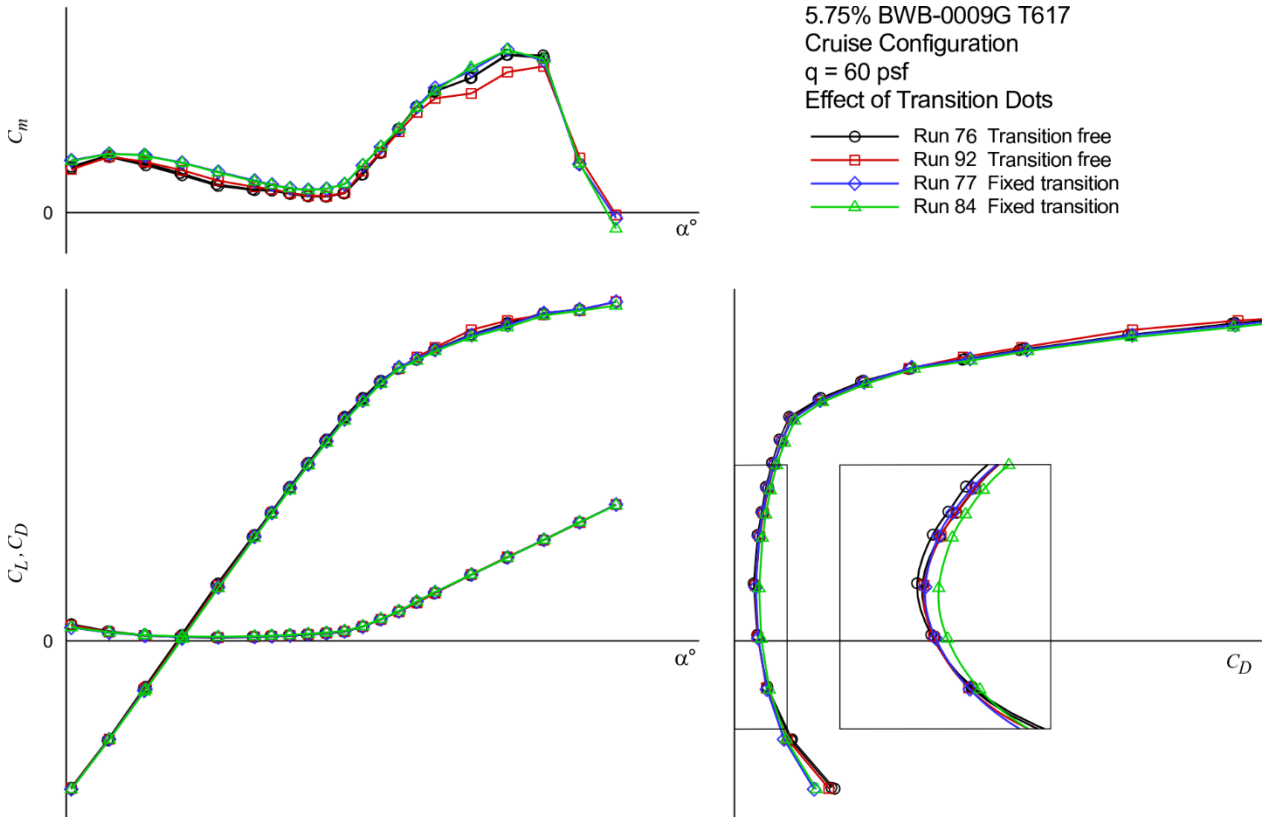

Fig. 19. Fixed transition effect on the longitudinal force and moment coefficients of the cruise configuration.

B. Cruise Configuration

Measurements with the model in the cruise configuration were obtained in both wind tunnels. The initial measurements checked for force and moment hysteresis with angle of attack as well as the effect of fixing the boundary layer transition with transition dots. Figure 19 shows a comparison of the transition fixed and transition free runs. The first transition free run (Run 76) was an increasing angle-of-attack sweep up to the maximum angle and then stepping back down, to check for hysteresis. No hysteresis was observed. Comparison the fixed and free transition runs show only a slight increase in pitching moment with fixed transition. A repeat transition free run (Run 92) showed some difference in pitching moment at the higher angles of attack.

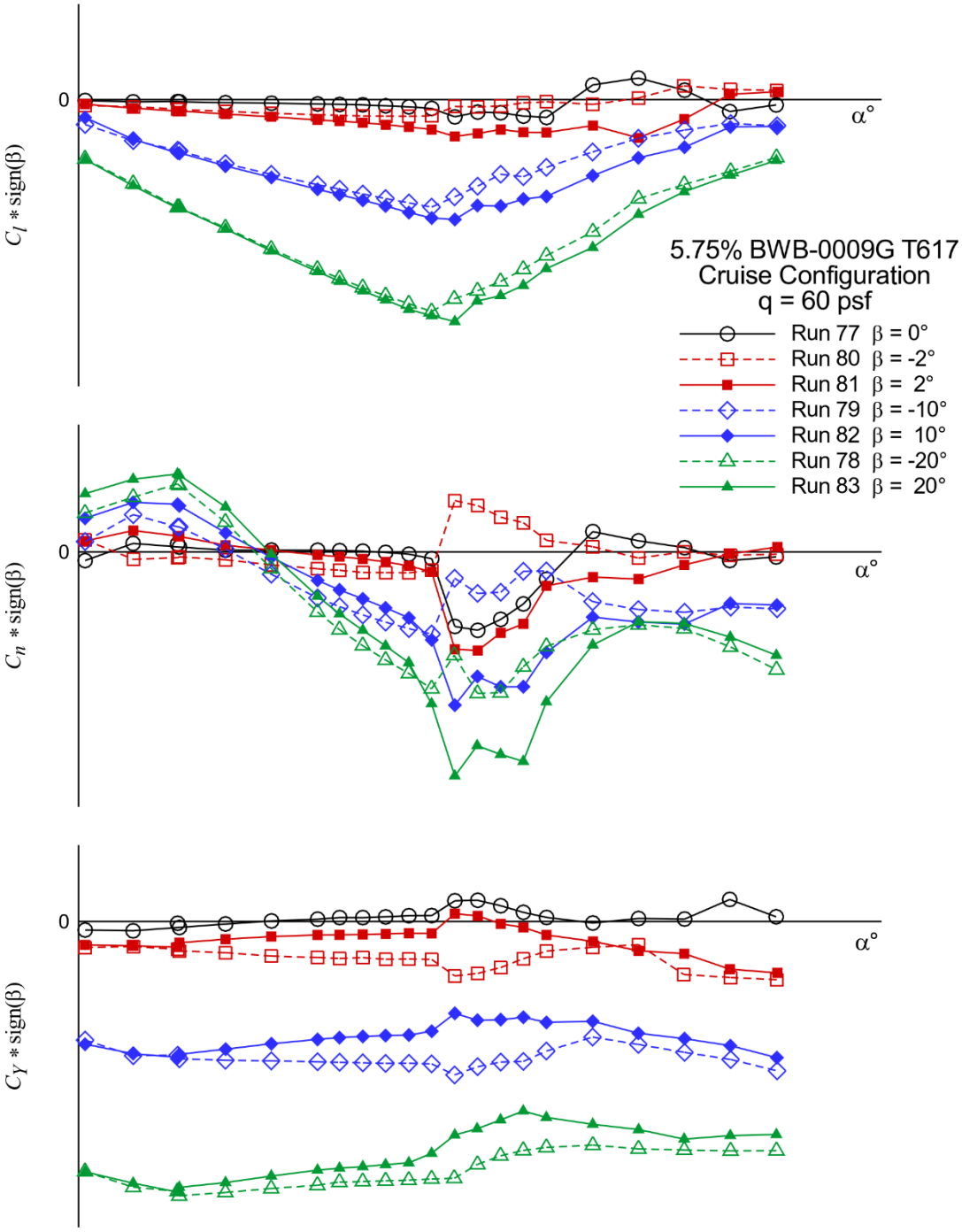

Fig. 20. Effect of sideslip on the lateral/directional force and moment coefficients of the cruise configuration.

The effects of sideslip angle on the lateral/directional coefficients of the cruise configuration are shown in Fig. 20. The data show some asymmetry in the model, particularly the side force data. This asymmetry was consistent between the two tunnels indicating that it is likely an asymmetry in the model and not the tunnel onset flow. The only designed model asymmetry is the rake in the right nacelle. The rolling moment and side force are fairly linear with angle of attack up to the pitch break angle. The yawing moment values are small and change sign with increasing angle of attack.

The lateral/directions sideslip derivatives for both the body and stability axes are shown in Fig. 21 for all three tunnel tests. The beta derivatives are consistent amongst the tests with the exception of a slight reduction in side force derivative from NFAC T078. The nearly neutral directional stability (C_{n_β}) is illustrated by the slightly stable values with increasing angle of attack in the stability axis and the slightly unstable values in the body axis.

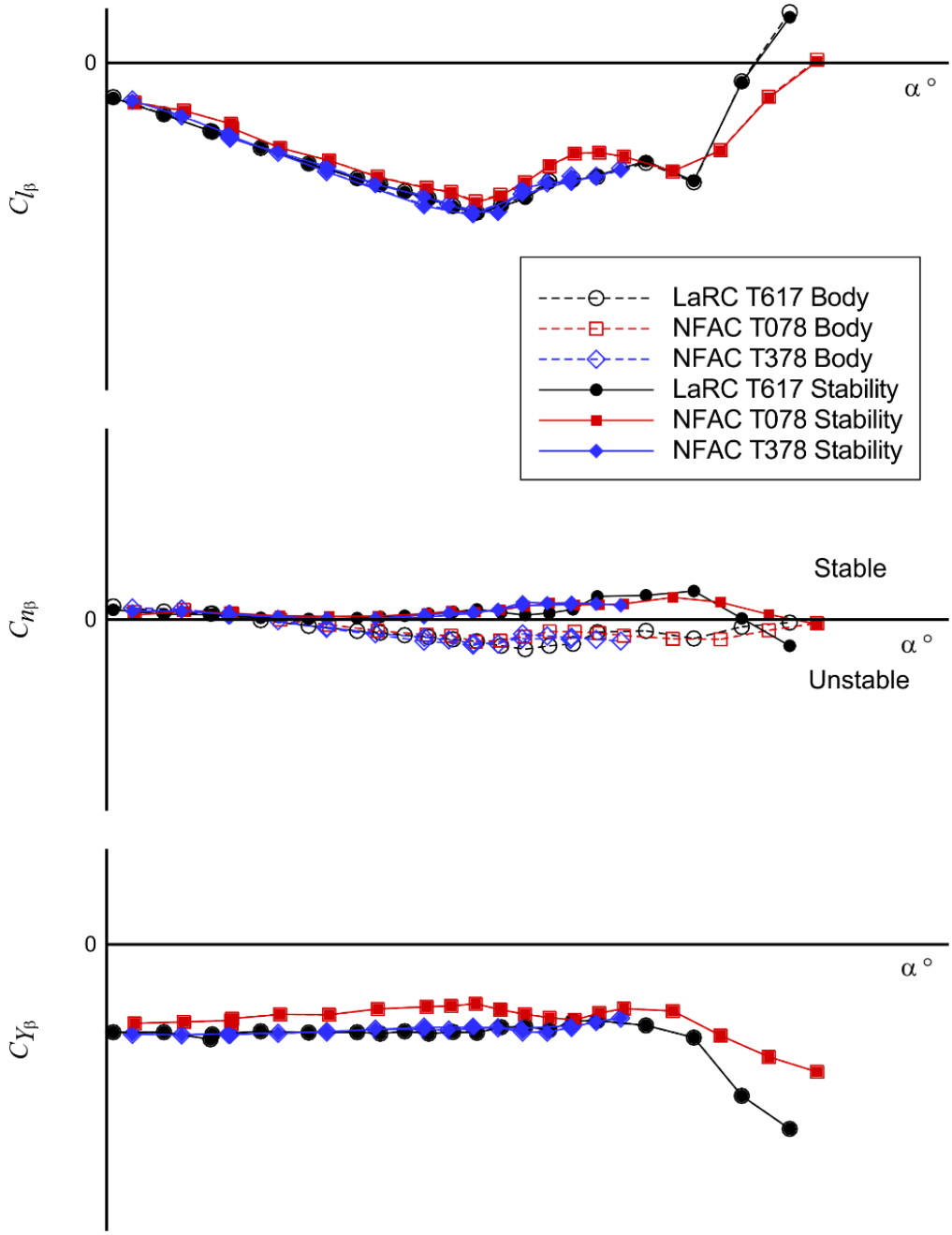

Fig. 21. Lateral/directional sideslip derivatives for the cruise configuration.

C. Takeoff & Landing Krueger Selection

A primary research objective of this series of tunnel tests was to establish the takeoff and landing Krueger settings for this configuration. The landing Krueger settings were evaluated by first establishing the center elevon (elevon 1/2) control effectiveness at a nominal landing Krueger setting. This elevon control effectiveness was then modeled and used to compute the trimmed (zero thrust) lift and drag values for each subsequent landing Krueger setting tested.

The elevon 1/2 control effectiveness model is shown in Fig. 22. The model was built from measurements at 0°, -10° and -40° of control deflection. The model assumes the control effectiveness is symmetric (+ or -) about zero deflection.

Examples of the landing Krueger setting measurements are shown in Figures 23 and 24. It is generally unclear from the measured values shown in Fig. 23 which setting will yield the best trimmed L/D shown in Fig. 24. For this deflection angle the minimum gap and overhang setting with the sealed slot (taped close) provided the best L/D. The max trimmed lift was generated at the mid gap and overhang position (2,2).

Determining the optimal Krueger setting for takeoff is more complex than the landing Krueger optimization. The takeoff and climb-out flight phases are untrimmed dynamic maneuvers. To determine the best Krueger setting for these maneuvers requires running a takeoff and climb-out simulation analysis using the aerodynamic measurements from the various Krueger configurations tested.

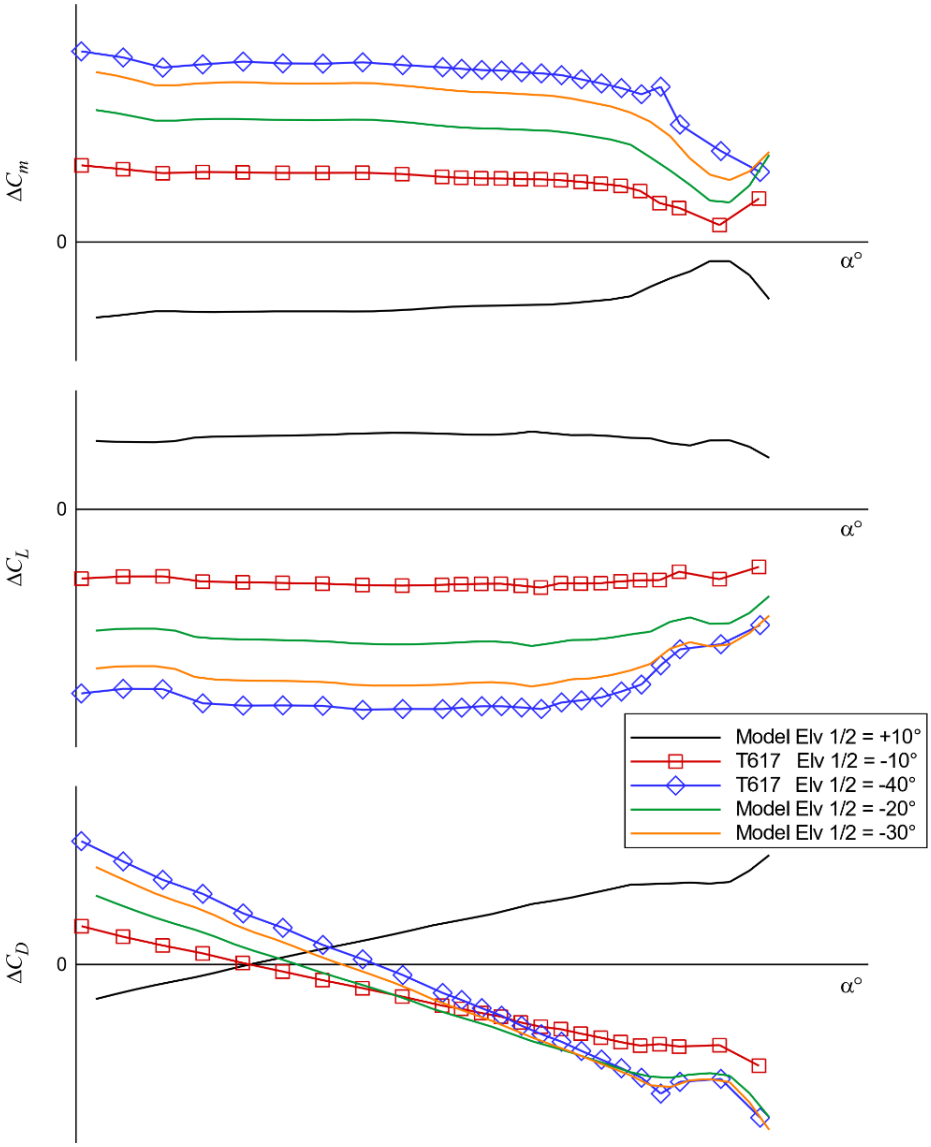

Fig. 22. Model of center elevon 1/2 control effectiveness.

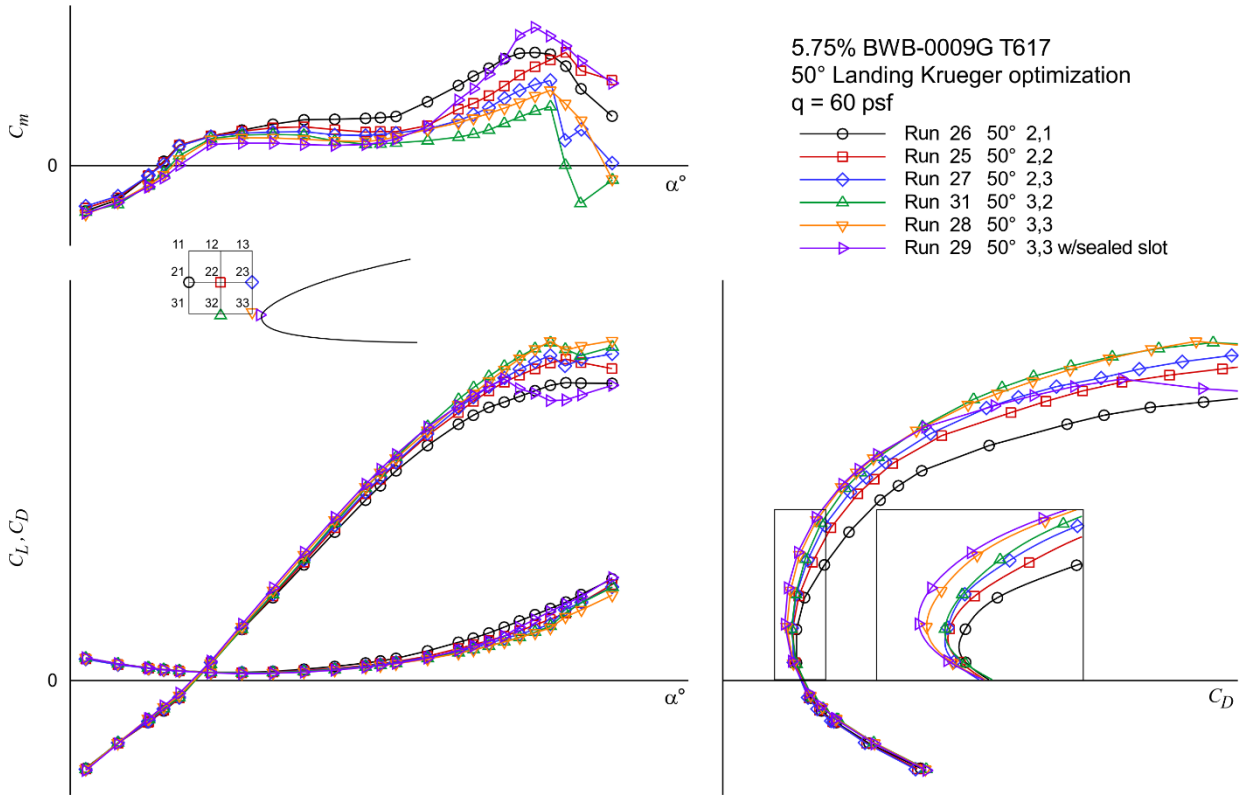

Fig. 23. Landing Krueger measurements for 50° deflection.

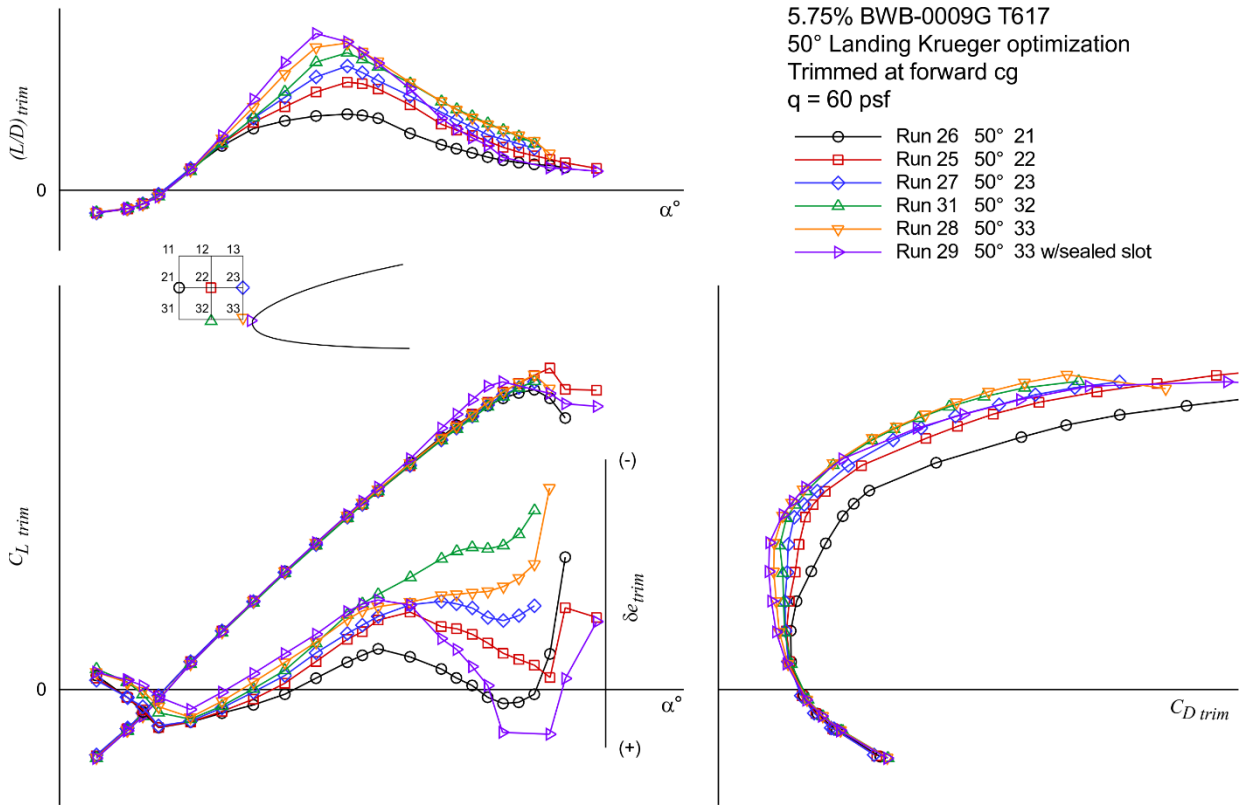

Fig. 24. Trimmed landing Krueger values for 50° deflection.

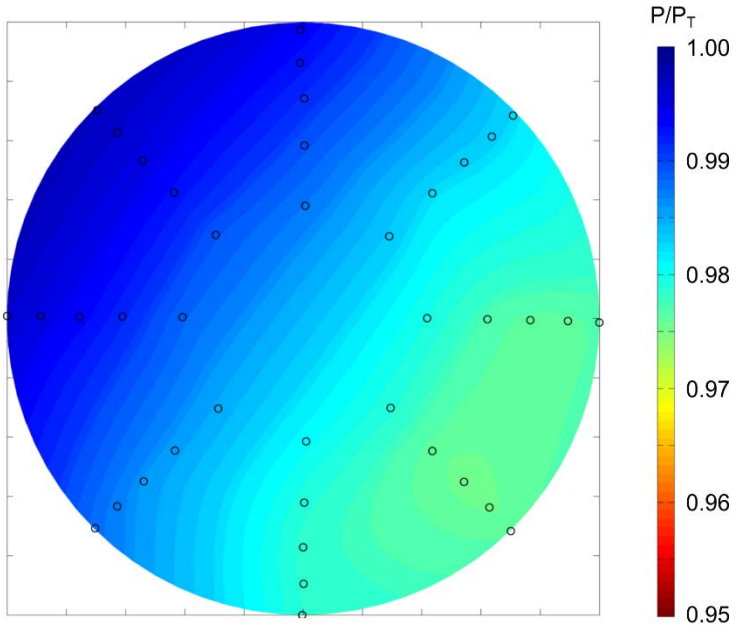

Fig. 25. Example total pressure ratio contour plot for the right engine nacelle (aft looking forward).

D. Flow-thru Inlet Distortion

The 40-probe pressure rake in the right nacelle, shown in Fig. 8, provided measurements of inlet distortion in terms of the measured to total pressure ratio. An example of the pressure ratio contour plots generated from these measurements at the various test conditions is shown in Fig. 25. This is a high angle of attack case with a slight positive sideslip. The pressure loss in the lower right corner of the nacelle (aft looking forward) is clearly evident.

Figures 26 and 27 show a collage of the pressure ratio contours plotted on an angle of attack and sideslip grid for the cruise configuration measurements of LaRC T617 and NFAC T078, respectively. Also shown on the figures are contour lines of constant pressure ratio. The figures show good agreement between the tests. Both test show that the distortion is worse on windward side and increases with angle of attack and sideslip. These results however are only the flow-thru nacelle mass flow conditions. They may provide some insight into the in-flow conditions but are not indicative of the engine induced mass flow conditions seen in flight.

Concluding Remarks

NASA collaborated with Boeing Research and Technology (BR&T) to conduct a series of wind tunnel tests on a new twin-engine Boeing BWB transport configuration. A 5.75-percent scale model was tested in two low-speed wind tunnels. This testing focused on the basic aerodynamics of the configuration and selection of the leading edge Krueger slat position for takeoff and landing.

The first test was conducted in the Langley 14- by 22-Foot Subsonic Tunnel with both the open and closed test section configuration. These data along with a considerable pre-test CFD effort have provided a significant data set for future low-speed tunnel correction analysis.

The subsequent two tests of the model in the NFAC 40- by 80-Foot Tunnel were conducted with different internal balances. Comparison of measurements from like conditions indicate that there may be an error in the gauge distances used in processing one of the balances. The calibrations of both balances are being checked in an effort to resolve the differences.

The lateral/directional measurements from both wind tunnels indicate that there is a slight asymmetry in the model. The only designed asymmetry is the pressure rake in the right nacelle. Analysis of the cruise configuration show a nearly neutral directional stability. Further investigation into the lateral/directions control effectiveness is warranted.

An extensive data set of leading edge Krueger deflection, gap and overhang characteristics was explored for both takeoff and landing conditions. From this data the takeoff and landing Krueger setting were selected and used in subsequent system analysis studies and follow-on inlet distortion and turbine propulsion-simulator tests.

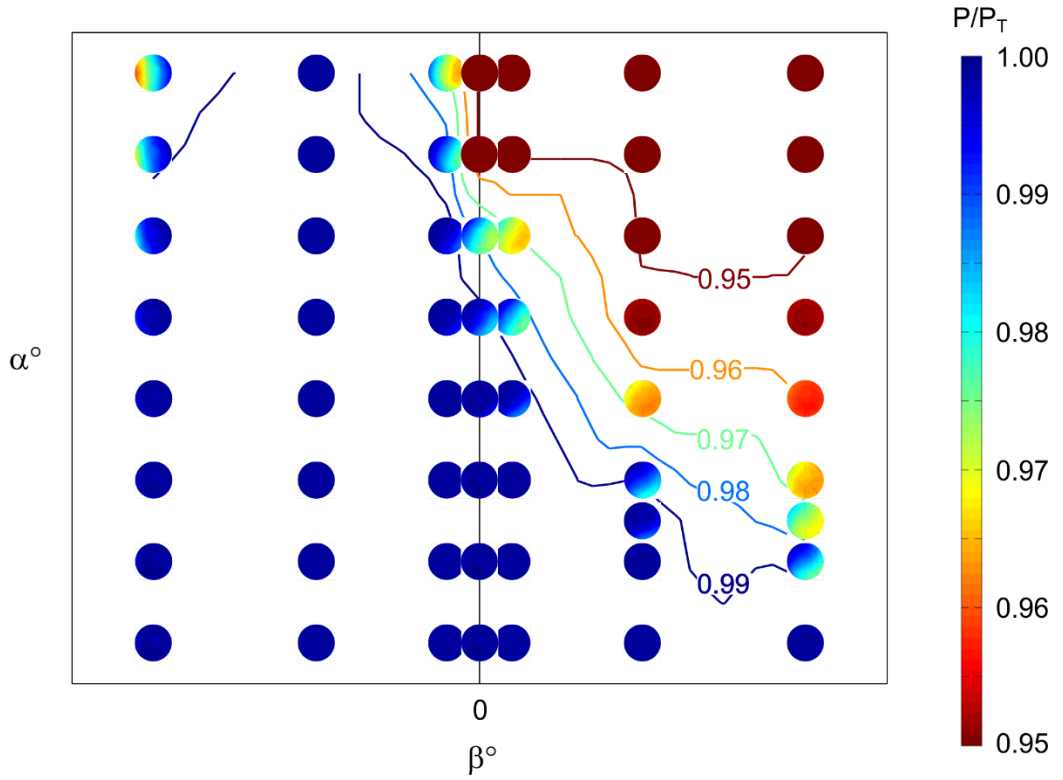

Fig. 26. Right nacelle total pressure ratio contours for the cruise configuration from 14x22 Test 617.

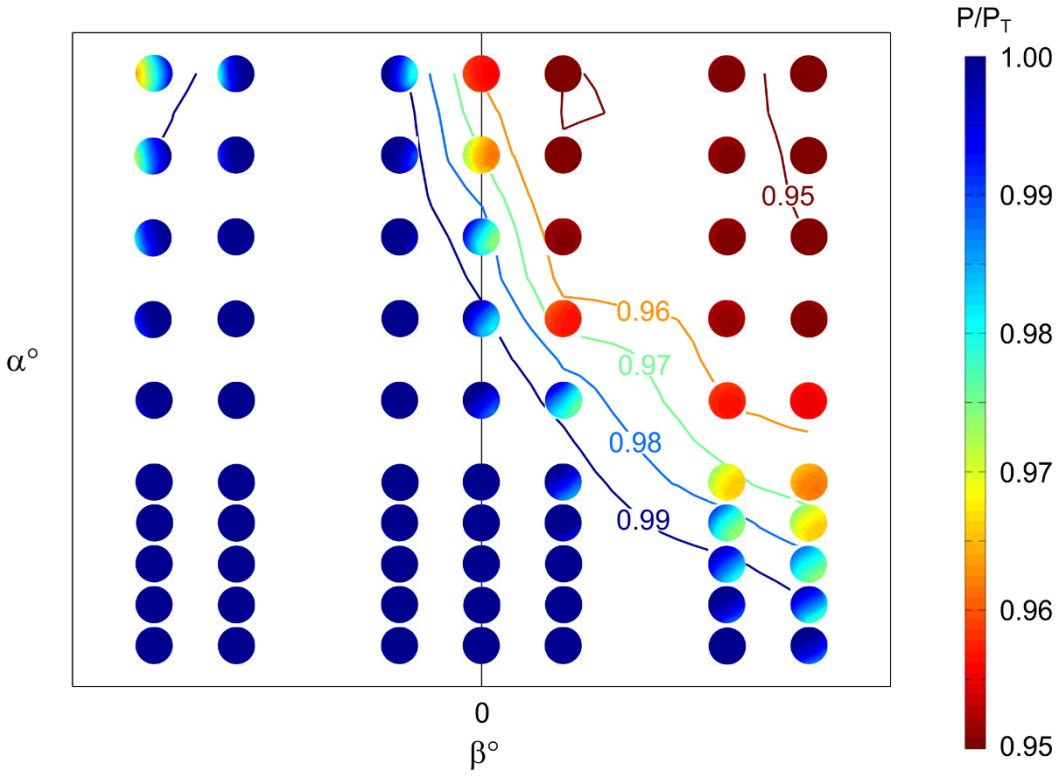

Fig. 27. Right nacelle total pressure ratio contours for the cruise configuration from NFAC Test 078.

Flow-thru inlet distortion measurements from right nacelle pressure rake show that the distortion is worse on windward side and increases with angle of attack and sideslip. These results however are only the flow-thru nacelle mass flow conditions. They may provide some insight into the on-flow conditions but are not indicative of the engine induced mass flow conditions seen in flight.

Final results and conclusions from these tests are pending the results of the balance calibration checks.

Acknowledgements

The authors would like to thank the test teams from the NASA Langley 14-by-22-Foot Subsonic Tunnel in Hampton, Virginia, and the National Full-Scale Aerodynamics Complex 40-by-80-Foot Tunnel, for their efforts in establishing this extensive dataset. Furthermore, they would like to thank all the members of ERA ITD-51A research team for their very fruitful discussions and cooperative work. The authors want to acknowledge the NASA Environmentally Responsible Aviation Project for sponsoring this research.

References

[1]Bonet, John T.; Schellenger, Harvey G.; Rawdon, Blane K.; Elmer, Kevin R.; Wakayama, Sean R.; Grown, Derrell L.; and Yueping Guo: *Environmentally Responsible Aviation (ERA) Project – N+2 Advanced Vehicle Concepts Study and Conceptual design of Subscale Test Vehicle (STV)*, NASA CR-2011-216519, December 2011.

[2]Roberts, Andrew C.; and Smith Kenneth M.: *Development Of A New Flow-Through Force Measurement Balance With Improved Accuracy For Use In Powered Wind Tunnel Model Testing*, AIAA 15th Aerodynamic Testing Conference, May 18-20, 1998, San Diego, CA, AIAA 1988-2059.

[3]American Institute of Aeronautics and Astronautics: *Recommended Practice: Calibration and Use of Internal Strain-Gage Balances with Application to Wind Tunnel Testing*, AIAA R-091-2003, January 2003.

[4]Gentry, G. L., Jr.; Quinto, P. F.; Gatlin, G. M.; and Applin, Z. T.: *The Langley 14- by 22-Foot Subsonic Tunnel: Description, Flow Characteristics, and Guide for Users*, NASA TP-3008, Sept. 1990.

[5]Herriot, John G.: *Blockage Corrections for Three-dimensional-Flow Closed-Throat Wind Tunnels, With Consideration of the Effect of Compressibility*, NACA Rep. 995, 1950.

[6]Quinto, P. Frank; and Orie, Nettie M.: *Langley 14- by 22-Foot Subsonic Tunnel Test Engineer's Data Acquisition and Reduction Manual*, NASA TM-4563, June 1994.